Carbohydrate Polymers 84 (2011) 709–712

Contents lists available at ScienceDirect

Carbohydrate Polymers

journal homepage: www.elsevier.com/locate/carbpol

An analysis of anisotropic gel forming process of chitosan

Toshiaki Dobashi[a,*], Naoko Tomita[a], Yasuyuki Maki[a], Chih Pong Chang[b], Takao Yamamoto[a]

[a] Department of Chemistry and Chemical Biology, Graduate School of Engineering, Gunma University, Tenjin-cho, Kiryu, Gunma 376-8515, Japan
[b] Department of Textile Engineering, Faculty of Engineering, Chinese Culture University, Taipei 11192, Taiwan

ARTICLE INFO

Article history:
Received 23 September 2009
Received in revised form 9 April 2010
Accepted 6 July 2010
Available online 13 July 2010

Keywords:
Chitosan
Anisotropic
Gel
Dialysis
Birefringence

ABSTRACT

We have prepared anisotropic chitosan gels with birefringence by immersing a sandwiched chitosan in aqueous acetic acid into aqueous sodium hydroxide. The gel forming process was traced under observation with crossed nicols and open nicols with and without litmus agent. The time courses of the gel front, the birefringent layer and the pH-change layer agreed with each other fairly well. The early stage of the dynamics was expressed by a theory with an assumption of an OH^- diffusion-limited process, whereas the behavior in the late stage deviated from the theoretical one. The deviation results from the effect of the outflow of protons, and the crossover of the two behaviors is attributed to the relaxation to the thermal equilibrium.

1. Introduction

Chitosan hydrogels are used in a variety of fields and are expected to develop further as drug carriers, vascular grafts, artificial cartilages, wound dressings, scaffolds as well as food additives, biosensors and adsorbents of harmful materials (Berger et al., 2004; Chen, 2008; Druly & Mooney, 2003; Peppas, Hilt, Khademhosseini, & Langer, 2006; Pilnik & Romboults, 1985). For each application, a variety of routes for preparation have been developed and improved; For example, layer-by-layer assembly for controlling blood coagulation (Sakaguchi, Serizawa, & Akashi, 2003), onion-like hydrogels for cell culture scaffolds (Ladet, David, & Domard, 2008). For the use of adsorbents and sensors of harmful materials, birefringent hydrogels could have an advantage in holding a large amount of harmful materials in the sizable interspace of the polymer network and of detecting the materials sensitively by a change in birefringence.

Recent studies of dialysis of concentrated rodlike and semiflexible polymer solutions showed that anisotropic gels are yielded with the dialysis of the polymer solutions into cross-linker solutions (Dobashi, Furusawa, Kita, Minamisawa, & Yamamoto, 2007; Dobashi, Nobe, Yoshihara, Yamamoto, & Konno, 2004; Maki et al., 2009). Chitosan aqueous solution is known to become a gel in alkaline solution without any chemical cross-linkers. Therefore, it is interesting to study the difference of the dynamics for the systems with cross-linkers and without cross-linkers, from both academic interest and application. In this study, as a first step of the development of anisotropic chitosan gels, we studied the gel forming process.

2. Experimental

Chitosan (chitosan 300, the degree of de-acetylation > 80%) was purchased from Wako Pure Chemicals, Co. Ltd., and the molecular weight M_w was determined to be 1.1×10^6 by measuring the intrinsic viscosity of chitosan in 0.25 M acetic acid/0.25 M sodium acetate with Mark-Houwink-Sakurada equation (Kasaai, Arul, & Charlet, 2000). Chitosan solution was prepared by dissolving the chitosan in 2 wt% acetic acid of analytical grade at 2 wt%. 6 mL of the solution was extruded into 50 mL of 0.3 M NaOH to prepare a hydrogel string, to examine the structure of hydrogels under crossed nicols, as shown in Fig. 1(a). To analyze the dynamics of anisotropic gelation, 200 μL of the chitosan solution was sandwiched between a set of cover glasses with a diameter of 15 mm, and immersed into 40 mL of 0.3 M NaOH to prepare a chitosan gel film, as shown in Fig. 1(c). The front lines of the turbid gel layer and the birefringent layer were traced under observation with open nicols and crossed nicols, respectively. To follow the pH change, a small amount of litmus reagent was added in the chitosan solution, and the interface between the pink zone (acidic) and sky blue zone (alkaline) was traced in the course of gelation. All the experiments were done at 25 °C using a water bath.

* Corresponding author. Tel.: +81 277 30 1427; fax: +81 277 30 1427.
E-mail address: dobashi@chem-bio.gunma-u.ac.jp (T. Dobashi).

0144-8617/$ – see front matter © 2010 Elsevier Ltd. All rights reserved.
doi:10.1016/j.carbpol.2010.07.004

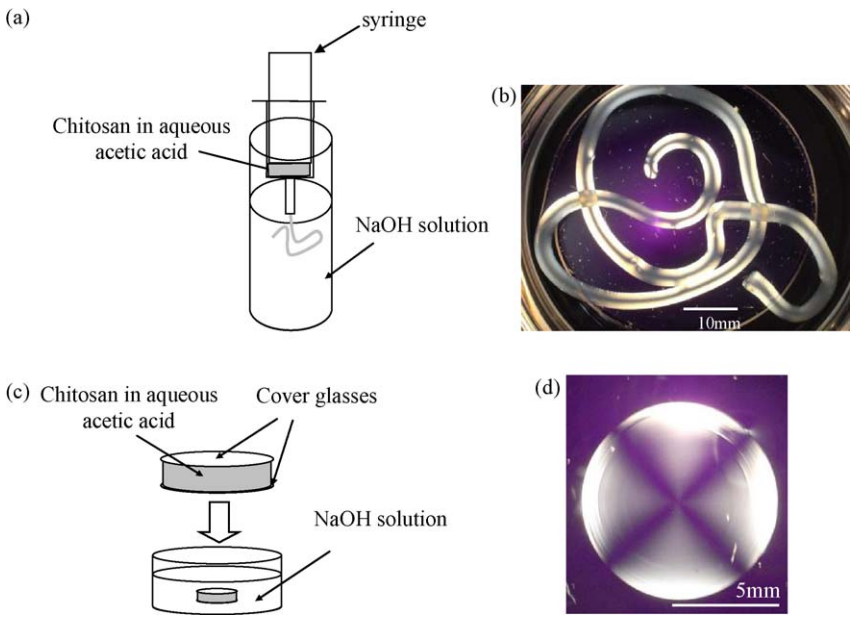

Fig. 1. The preparation procedure of chitosan hydrogel strings (a) and films (c). The photo images observed under crossed nicols for strings and films are shown in (b) and (d), respectively.

3. Results and discussion

At the very initial process of immersion for preparing both hydrogel strings and films, cross-links occur at the interface between the inner chitosan solution and the outer sodium hydroxide solution, and the resultant thin membrane plays the role of semipermeable (dialysis) membrane: permeable to water and ions and impermeable to chitosan molecules. Fig. 1(b) shows the photo image after the complete gelation observed under crossed nicols. We observe clear black cross-lines in the regions where two tubes are superposed. Black cross-lines are also observed in the gel films, as shown in Fig. 1(d). These images cannot be explained only by the difference of relative strength of birefringence between the outer and inner parts of the gel. This kind of image is consistent with an orientation of domains such as polymer aggregates. According to the optics (Born & Wolf, 1974) based on the direction of the vibration of the incident light against the sample, the images under crossed nicols for the sample are summarized as follows: (1) arranged with radial axis of symmetry; light transmits through the string near the edge than near the center, (2) circumferentially arranged; light transmits through the string near the center than near the edge, and (3) arranged along the string length; light transmits through any parts of the string, especially stronger near the center. As shown in Fig. 1(b) observed under the crossed nicols, more light transmits through the gel string near the edge, which indicates arrangement of (1), which is the same as the case of curdlan, etc. In the latter, the direction of the symmetrical axis was confirmed by X-ray scattering. The average directions of chitosan molecules or chitosan-rich domains of the strings and the films are assumed to be the same.

In the course of the gel forming process by means of the sandwich method, all the front lines of gelation, orientation and pH-change proceeds simultaneously, as shown in Fig. 2. The mechanism of the synchronization of the motion of the front lines could be related to the gradient of the chemical potential of chitosan near the boundary layer, but is not clear at this stage.

In the case of Curdlan solution and DNA solution studied previously, multivalent cations played the role of the cross-linkers and the dynamics of gel forming process was limited by the diffusion of the cations. In the case of chitosan, the immersing solution does not contain such cross-linkers. When the pH of chitosan solution is high, the positive charges of chitosan molecules are neutralized and undergoes coacervation-phase inversion, and chitosan gels. The physical cross-links correspond to the formation of hydrophobic interactions and hydrogen bonding between chain segments (for example, Montembault, Viton, & Domard, 2005a). The threshold pH required for chitosan gelation is known in the range between pH 5 and pH 8, but depends on the condition such as the molecular weight and the degree of de-acetylation of chitosan and chitosan concentration (Montembault, Viton, & Domard, 2005b). The synchronization of the motion of the three front lines enables us to examine the dynamics of the gel forming process by tracing one of them. Then we tried to make an analysis for the gel front line based

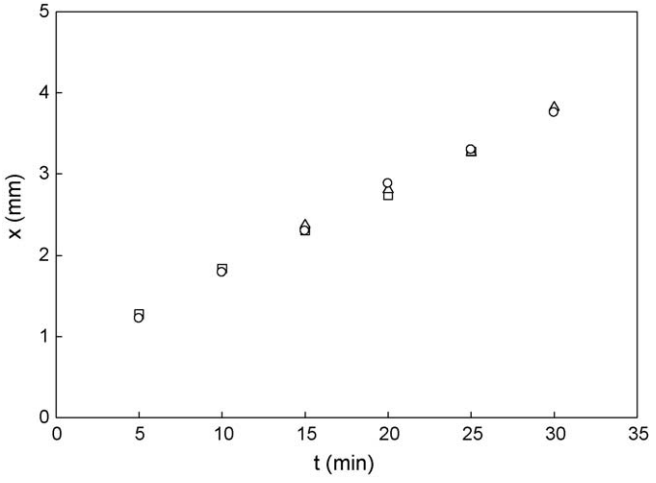

Fig. 2. Time course of the distance from the edge of the cover glass to the interface between the gel layer and the sol core observed under open nicols (gel thickness) (○), to the interface between anisotropic layer and isotropic core observed under crossed nicols (birefringent layer thickness) (□), and to the interface between the pink layer and the sky blue core colored by litmus agent (△) (high-pH layer thickness) in the immersing process of 200 μl of chitosan solution (1 wt% chitosan in 1 wt% aqueous acetic acid with 0.05 g/dl litmus agent) in 40 mL of 0.3 M NaOH. (For interpretation of the references to color in this figure legend, the reader is referred to the web version of the article.)

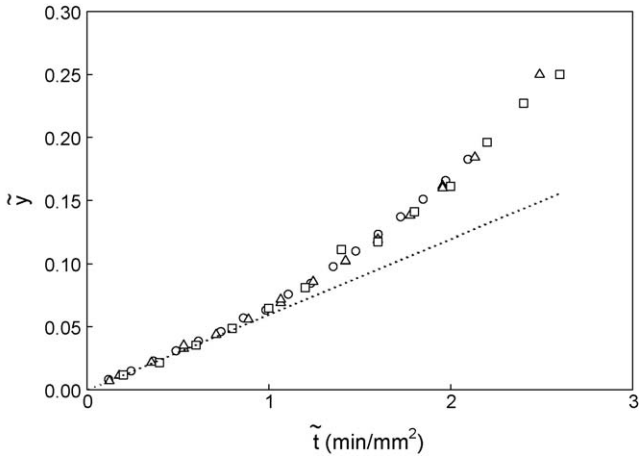

Fig. 3. Time course of gel thickness in a scaled plot. The diameters of the cover glasses are 12 mm (□), 15 mm (△) and 18 mm (○).

on a theoretical consideration (Nobe, Dobashi, & Yamamoto, 2005). The main assumptions and the theoretical results are summarized as follows. The assumptions applied for the present system are (a) All OH^- flowing into the inner chitosan solution are used to produce a gel layer. (b) The gel layer does not capture the OH^- as a sink; i.e., all the OH^- flowing into the gel layer arrive at the inner chitosan solution to keep a steady state. Under the above assumptions, only the motion of the boundary between the gel layer and the sol core is required to express the time course of gelation (the moving boundary picture for the dynamics of gel formation). Expressing the boundary motion in terms of the gel layer width $x = x(t)$ and introducing the scaled width $\tilde{x} = x/R$ and the scaled immersion time $\tilde{t} = t/R^2$, we have:

$$\tilde{y}(\tilde{x}) = K\tilde{t}, \tag{1}$$

where $\tilde{y}(\tilde{x})$ is the universal function of $\tilde{x}$ given by:

$$\tilde{y}(\tilde{x}) \equiv \frac{1}{2}(1-\tilde{x})^2\ln(1-\tilde{x}) - \frac{1}{4}\tilde{x}^2 + \frac{1}{2}\tilde{x}, \tag{2}$$

K is a constant related to the diffusion coefficient of OH^- In the case of dilute immersing solution, $\tilde{D}_{OH}$ is approximated as:

$$\tilde{D}_{OH} \approx \frac{\rho_g}{\rho_s}K \tag{3}$$

where ρ_g, and ρ_s are the OH^- concentration required for gel formation and the concentration of OH^- in the immersing solution, respectively. According to Eq. (1), we plotted the scaled function as in Fig. 3. The early stage is expressed as a line, suggesting that it is the OH^--diffusion-limited process, as assumed in the theory. The deviation from the theory in the late stage should be attributed to the relative proton transport from the inner chitosan solution into the outer immersing solution.

Let us discuss the proton flow from the view point of the relaxation process of the proton concentration in the inner solution and the deviation from the OH^--diffusion-limited picture. The proton concentration difference between the inner solution and the outer immersing solution at time t is denoted by $C(t)$. Since the flux of the proton flow $j(t)$ is proportional to the gradient of the proton concentration, we have:

$$j \approx \Gamma\frac{C(t)}{x(t)} \tag{4}$$

where Γ is a positive constant. Then, the relaxation behavior of the proton concentration in the inner solution is expressed as:

$$\pi(R-x)^2\frac{dC(t)}{dt} = -2\pi Rj = -2\pi R\Gamma\frac{C(t)}{x(t)} \tag{5}$$

The solution of the equation is obtained as:

$$C(\tilde{t}) = C_{in}\exp(-2\Gamma\tilde{u}(\tilde{t})) \tag{6}$$

where C_{in} is the initial proton concentration difference and:

$$\tilde{u}(\tilde{t}) = \int_0^{\tilde{t}} \frac{1}{\tilde{x}(\tilde{t})(1-\tilde{x}(\tilde{t}))^2}\,d\tilde{t} \tag{7}$$

Note that the expression (6) is denoted only in terms of the scaled variables. Hence, independently of the radius R, the time course of the gel front line expressed in terms of the scaled variables sits on a master curve. This scaling behavior agrees with the experimental result shown in Fig. 3.

In the small $\tilde{x}$ region (thus, in the small $\tilde{t}$ region), $\tilde{x}(1-\tilde{x})^2 \approx \tilde{x}$ and $\tilde{x}(\tilde{t}) \approx \sqrt{2K\tilde{t}}$ (see Eq. (2)), we have a stretched exponential type relaxation behavior:

$$C(\tilde{t}) = C_{in}\exp(-\sqrt{\tilde{t}/\tilde{\tau}}) \tag{8}$$

where the characteristic scaled time $\tilde{\tau}$ is given by $\tilde{\tau} = K/(8\Gamma^2)$. This expression leads to the following results;

(a) In the early stage $\tilde{t} < \tilde{\tau}$, the proton concentration is regarded to be equal to that at $\tilde{t} = 0$ and the OH^- concentration required for gel formation is maintained constant. Hence, time development of $\tilde{x}$ is well expressed by Eq. (2).
(b) In the late stage $\tilde{t} > \tilde{\tau}$, the concentration rapidly decreases and the OH^- concentration required for gel formation also decreases. Then, in this stage, the proton flow affects the gel formation process and the time development of $\tilde{x}$ deviates from the expression (2).

These results agree with the experimental data. From Fig. 3, we could estimate $\tilde{\tau}$ and K as $\tilde{\tau} \approx 1.0\text{min/mm}^2$ and $K \approx 5.9\times10^{-2}\,\text{mm}^2/\text{min}$. Then, we have $\Gamma \approx 8.6\times10^{-2}\,\text{mm}^2/\text{min}$. $\tilde{\tau}$ is proportional to K and K is proportional to ρ_s from Eq. (3). Since Eq. (2) holds in the time range $\tilde{t} < \tilde{\tau}$, to obtain the proportional relationship between $\tilde{y}$ and $\tilde{t}$ in the whole experimental range, $\tilde{\tau}$ need to be at least twice as large as the present case according to Fig. 3. Therefore, we could estimate that when the NaOH concentration in the immersing solution is larger than 0.6 M, the proton flow is negligible in the gel formation process.

In conclusion, we could prepare an anisotropic chitosan hydrogel film by a sandwich method. The pH change, gelation and birefringence occurred simultaneously. The early stage was explained well by a theory with the assumption of OH^--limited diffusion process. The deviation form the theory in the late stage was discussed on the basis of the relaxation phenomenon of the proton concentration of the chitosan solution.

Acknowledgments

This work was partly supported by Grant-in-Aid for Science Research from JSPS (#19540426 and #20656129), and by Grant-in Aid for Scientific Research on Priority Area "Soft Matter Physics" from the Ministry of Education, Culture, Sports, Science and Technology of Japan.

References

Berger, J., Reist, M., Mayer, N. M., Felt, O., Peppas, N. A., & Gurny, R. (2004). Structure and interactions in covalently and ionically crosslinked chitosan hydrogels for biomedical applications. *European Journal of Pharmaceutics and Biopharmaceutics*, *57*, 19–34.
Born, M., & Wolf, E. (1974). *Principles of Optics, Ver. 5*. Oxford, London: Pergamon Press.
Chen, R. H. (2008). Preparation, characteristics and applications of chitinous hydrogels. *Transactions of the Materials Research Society of Japan*, *33*(2), 417–424.

Dobashi, T., Nobe, M., Yoshihara, H., Yamamoto, T., & Konno, A. (2004). Liquid crystalline gel with refractive index gradient of curdlan. *Langmuir, 20*, 6530–6534.
Dobashi, T., Furusawa, K., Kita, E., Minamisawa, Y., & Yamamoto, T. (2007). DNA liquid crystalline gel as adsorbent of carcinogenic agent. *Langmuir*, *23*, 1303–1306.
Druly, J. L., & Mooney, D. J. (2003). Hydrogels for tissue engineering: scaffold design variables and applications. *Biomaterials*, *24*, 4337–4351.
Kasaai, M. R., Arul, J., & Charlet, G. (2000). Intrinsic viscosity–molecular weight relationship for chitosan. *Journal of Polymer Science, Part B. Polymer Physics Edition*, *38*, 2591–2598.
Ladet, S., David, L., & Domard, A. (2008). Multi-membrane hydrogels. *Nature*, *452*, 76–80.
Maki, Y., Wakamatsu, M., Ito, K., Furusawa, K., Yamamoto, T., & Dobashi, T. (2009). Optical anisotropy of calcium-induced alginate gels. *Journal of Biorheology*, *23*, 24–28.
Montembault, A., Viton, C., & Domard, A. (2005a). Physico-chemical studies of the gelation of chitosan in a hydroalcoholic medium. *Biomaterials*, *26*, 933–943.
Montembault, A., Viton, C., & Domard, A. (2005b). Rheometric study of the gelation of chitosan in aqueous solution without cross-linking agent. *Biomacromolecules*, *6*, 653–662.
Nobe, M., Dobashi, T., & Yamamoto. (2005). Dynamics in dialysis process for liquid crystalline gel formation. *Langmuir*, *21*, 8155–8160.
Peppas, N. A., Hilt, J. Z., Khademhosseini, A., & Langer, R. (2006). Hydrogels in biology and medicine: From molecular principles to bionanotechnology. *Advanced Materials*, *18*, 1345–1360.
Pilnik, W., & Romboults, F. M. (1985). Polysaccharides and food processing. *Carbohydrate Research*, *142*, 93–105.
Sakaguchi, H., Serizawa, T., & Akashi, M. (2003). Layer-by layer assembly on hydrogel surfaces and control of human whole blood coagulation. *Chemistry Letters*, *32*(2), 174–175.